

## Effect of purification treatment on corrosion resistance of Mg-Gd-Y-Zr alloy

WANG Jie, YANG Yuan-sheng, TONG Wen-hui

Institute of Metal Research, Chinese Academy of Sciences, Shenyang 110016, China

Received 25 September 2010; accepted 20 December 2010

**Abstract:** Mg-Gd-Y-Zr alloys were purified by filtering purification with and without vacuum. The type, morphology, size distribution and volume fraction of inclusion were analyzed with OM and SEM. The effect of inclusion in Mg-Gd-Y-Zr alloys on anticorrosion ability was investigated with salt spray test and electrochemical test. The results show that the inclusions in the alloy can be removed effectively by filtering purification. The average size of inclusions in the alloys is decreased from 12.7  $\mu\text{m}$  to 2.0  $\mu\text{m}$  and the volume fraction of inclusions is reduced from 0.30% to 0.04%. With the decrease of the size of inclusions in the alloys, the corrosion rate of the alloys decreases dramatically from 38.8  $\text{g}/(\text{m}^2\cdot\text{d})$  to 2.4  $\text{g}/(\text{m}^2\cdot\text{d})$  in the salt spray test. The corrosion potential increases while the corrosion current decreases and the polarization resistance increases in the electrochemical tests, which indicates that the anticorrosion ability is improved.

**Key words:** Mg-Gd-Y-Zr alloy; filtering purification; inclusion; corrosion rate; polarization curve; polarization resistance

### 1 Introduction

In the past decades, magnesium alloys containing heavy rare earth elements have shown great potential for structural application in automotive, aircraft and aerospace industries. Recently, many investigations have been conducted concerning the microstructure and mechanical properties of Mg-Gd-Y-Zr alloys due to their higher specific strength and better creep resistance compared with traditional commercial Mg-Al based alloys[1–3]. However, during the smelting and casting processing, magnesium and rare earth elements are prone to oxidize rapidly, which results in the loss of rare earth elements and the formation of inclusions[4–5]. These inclusions generally deteriorate the continuity of the magnesium matrix by forming the defects such as pores and cracks, which are detrimental for the mechanical properties and corrosion resistance of the alloys[6–7]. Several refining methods have been developed, including traditional flux refining and fluxless refining, such as inert gas, vacuum distillation refining and filtering refining[8–12]. Traditional flux refining method is considered one of the most effective ways to remove the inclusions in magnesium alloys. However,  $\text{MgCl}_2$  in the flux is prone to react with the rare earth elements Gd and Y, producing new flux inclusions and consuming Gd and

Y elements[13–14], which will deteriorate the mechanical properties and corrosion resistance. Therefore, it is necessary to seek effective purification treatments to reduce or eliminate inclusions in the Mg-Gd-Y-Zr alloys. According to the previous research[15], filtering purification should be an effective purification method to avoid the formation of new inclusions and loss of rare earth elements. Furthermore, under vacuum condition, this purification treatment has more favorable effects on the purity of alloys. In addition, filtering purification is more environment-friendly in comparison with flux refining method.

In this work, a series of alloys containing inclusions with different sizes were prepared by filtering purification treatments. The effect of the filtering purification was examined and evaluated, aiming to further understand the relationship between the size of inclusions and the corrosion behavior in the Mg-Gd-Y-Zr alloys.

### 2 Experimental

In the present study, the chemical compositions of Mg-Gd-Y-Zr alloy studied were Gd12.07%, Y3.27%, Zr0.38%, Fe<0.001%, Cu0.001%, Ni <0.001% (mass fraction) and Mg balance. The alloys were melted in an electric resistance furnace at 750 °C under the protection

of mixed 0.5% SF<sub>6</sub> and 99.5% CO<sub>2</sub> gas (volume fraction). The melt was poured into a graphite mould through stainless steel nets preheated to 720 °C. The dimension of the ingot was  $d48\text{ mm} \times 80\text{ mm}$ .

The dimensions of specimens for salt spray tests were 25 mm×15 mm×4 mm. After being polished up to 2000 grit, the total surface area ( $S$  in cm<sup>2</sup>) and mass ( $m_0$  in g) of the specimens were measured. According to ASTM B117[16], the corroded specimens were exposed into the salt spray chamber. After 6 d( $t$ ), the corroded specimens were cleaned in a solution of 15% Cr<sub>2</sub>O<sub>3</sub> + 1% AgNO<sub>3</sub> (volume fraction) in 500 mL water, and then were rinsed by acetone and distilled water and dried. The mass of the corroded specimen ( $m_c$  in g) was measured by an analytical balance. Then the mass loss ( $m_L$  in g) and the corrosion rate ( $R$  in g/(m<sup>2</sup>·d)) were calculated by the following equations:

$$m_L = m_0 - m_c \quad (1)$$

$$R = m_L / (St) \quad (2)$$

Electrochemical polarization experiments were carried out using a Potentiostat/Galvanostat Model 2273A. The specimens were metallographically polished prior to each experiment, followed by washing with distilled water and acetone. The surface area that was exposed to the solution was about 1 cm<sup>2</sup>. Polarization tests were carried out in a corrosion cell containing 500 mL of 3.5% (mass fraction) NaCl solution, and a

standard three-electrode system was used with saturated calomel electrode (SCE) as a reference electrode, a platinum electrode as counter electrode and the sample as working electrode. Specimens were immersed into the test solution and a polarization scan was carried out at a rate of 0.2 mV/s after a steady state potential was achieved.

The morphology of nonmetallic inclusions in the ingots was observed using optical microscope (OM). The size and volume fraction of nonmetallic inclusions were measured with the SISC-IAS image software. The morphology of the corroded surface was characterized using scanning electron microscope (SEM). The composition of nonmetallic inclusions was analyzed by energy dispersive spectroscope (EDS) attached to the SEM.

### 3 Results and discussion

#### 3.1 Purifying effectiveness

The main morphology of nonmetallic inclusions in the alloy was clarified in previous work[15]. The inclusions in the alloy without purification have irregular shape and exist in the form of cluster. After the purification treatment, the distribution of finer inclusions got more dispersed. The composition of the main inclusions was analyzed by EDS, as shown in Fig.1. The

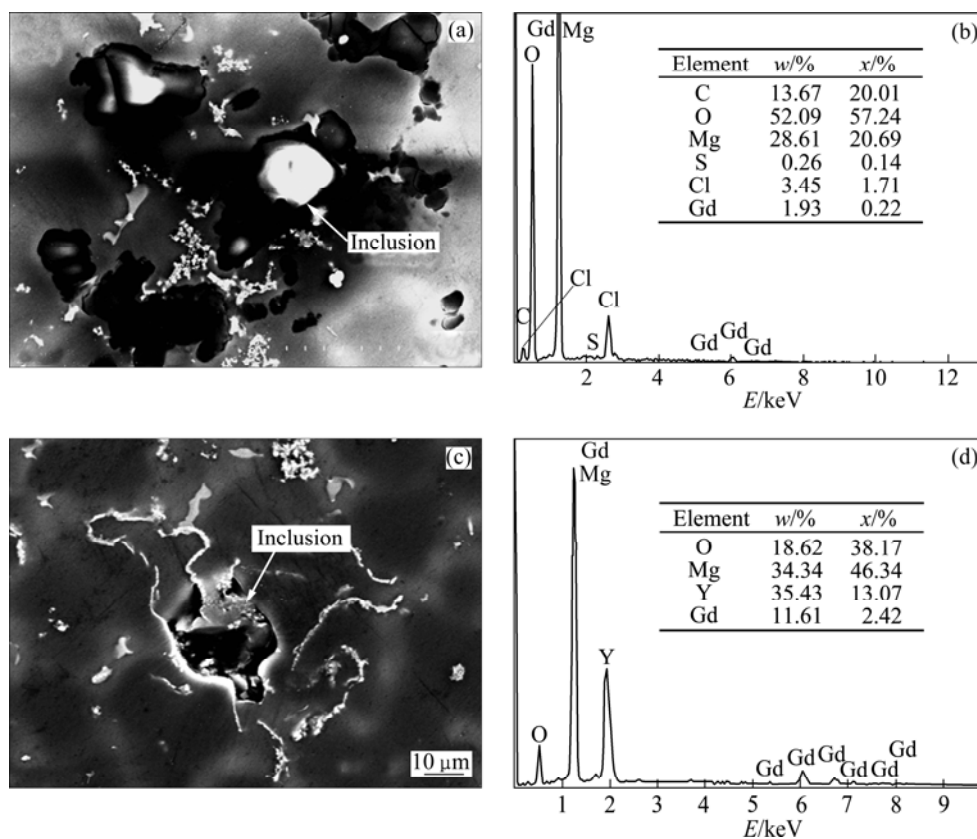
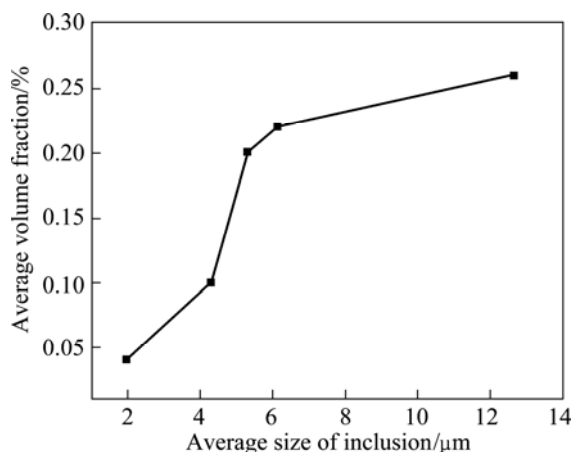


Fig.1 SEM images and EDS analyses of inclusions in Mg-Gd-Y-Zr alloy: (a), (b) Flux-inclusion; (c), (d) Oxide

results show that non-metallic inclusions are mainly composed of MgO, chlorides and oxides of Gd and Y. The presence of MgCl<sub>2</sub> in inclusions, detected by EDS, demonstrates the existence of flux-inclusions.

After purification treatments, some samples with different inclusions content were analyzed, and the statistical results of the average size and volume fraction of inclusions in the alloys are shown in Fig.2. The average size of the inclusions in the sample without purification treatment is 12.7  $\mu\text{m}$ , and the average sizes of the inclusions in purified samples are 6.1, 5.3, 4.7 and 3.2  $\mu\text{m}$ , respectively. When the alloy was prepared and purified in vacuum, the average size of the inclusions in the alloy decreases from 12.7  $\mu\text{m}$  to 2.0  $\mu\text{m}$  and the average volume fraction of inclusions is reduced from 0.30% to 0.04%. The results are improved under the optimized condition, as shown in Fig.2, compared with the average size (4.3  $\mu\text{m}$ ) and volume fraction (0.1%). Based on the results, it can be concluded that the purifying effectiveness under the condition of vacuum is better than that under the protective atmosphere.



**Fig.2** Relationship between average size and average volume fraction of inclusions

Distribution of inclusions in the samples with different inclusion contents is shown in Fig.3, which shows that the distribution of nonmetallic inclusions in different size ranges changes in a large range with different inclusion contents. For the unpurified alloy, the nonmetallic inclusions larger than 10  $\mu\text{m}$  distribute equably. The inclusion with size larger than 100  $\mu\text{m}$  can even be found in the unpurified alloy. When the average size of inclusions is smaller than 10  $\mu\text{m}$ , the size distribution of nonmetallic inclusions is similar and the frequency of inclusions smaller than 10  $\mu\text{m}$  increases. Under the vacuum condition, the frequency of inclusions smaller than 10  $\mu\text{m}$  reaches 96% and the frequency of inclusions larger than 5  $\mu\text{m}$  is reduced to 4%. Therefore, the statistical results are consistent with the metallography of the alloy[15], which confirms that the

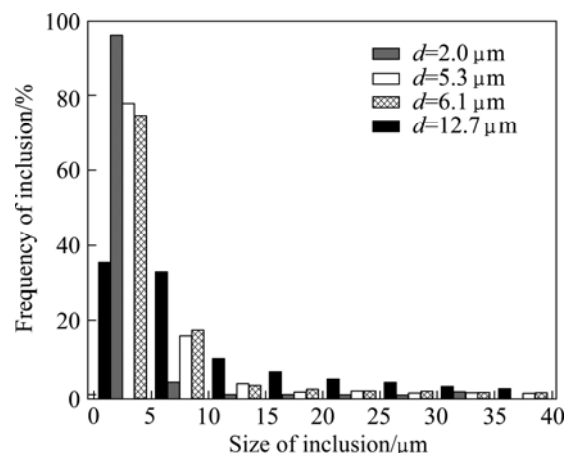


**Fig.3** Distribution of inclusions in alloys with different average sizes of inclusions ( $d$ : average size of inclusions)

size of inclusions in the alloy can be reduced effectively by purification.

### 3.2 Corrosion resistance

The morphological characteristics of the corroded specimens in the salt spray test are shown in Fig.4. It can be seen that deep corrosion pits are distributed on the surface of specimens, which contains large inclusions. The decrease of the average size of inclusions is effective on the improvement of the corrosion resistance of the alloy. The corrosion rates of the alloys containing inclusions are shown in Fig.5. Under as-cast condition, with the decrease of the average size and volume fraction of inclusions, the corrosion resistance is improved. When the average size and volume fraction of inclusions decrease from 12.7  $\mu\text{m}$  and 0.26% to 4.3  $\mu\text{m}$  and 0.06%, respectively, the corrosion rate of the alloy decreases dramatically from 38.8  $\text{g}/(\text{m}^2\cdot\text{d})$  to 2.5  $\text{g}/(\text{m}^2\cdot\text{d})$ . When the average size and volume fraction of inclusions are further decreased to 2.0  $\mu\text{m}$  and 0.04%, respectively, the corrosion rate of the alloy prepared under the vacuum condition decreases to 2.4  $\text{g}/(\text{m}^2\cdot\text{d})$ , which is the lowest corrosion rate. The deleterious effects of inclusions on corrosion resistance of magnesium alloy can be attributed to the formation of galvanic coupling between the inclusions and magnesium matrix[17], which accelerates the corrosion rate. The decreases of inclusions improve the corrosion resistance of the alloy by reducing the cathode areas. Therefore, the alloys with purification treatment exhibit excellent corrosion resistance.

The potentiodynamic polarization curves of Mg-Gd-Y-Zr alloy are shown in Fig.6. The polarization curves reveal that the impact of inclusion size is significant in the cathode kinetics towards decreased rates. The cathode part of the curve exhibits that the cathode currents decrease with the decrease of the

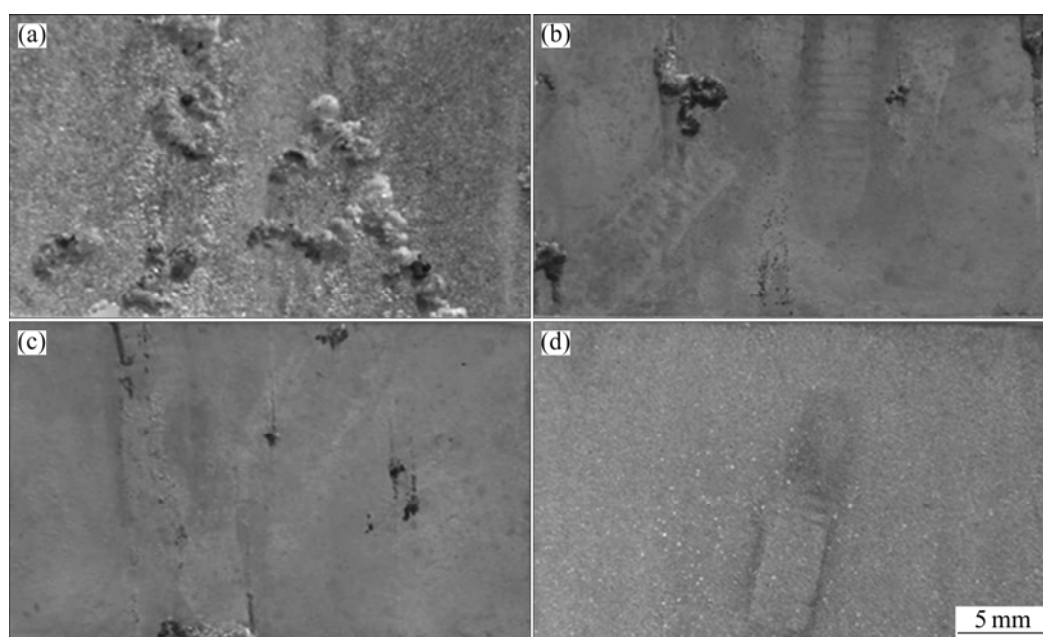


**Fig.4** Corrosion morphologies of Mg-Gd-Y-Zr alloys with different average sizes of inclusions: (a)  $d=12.7 \mu\text{m}$ ; (b)  $d=6.1 \mu\text{m}$ ; (c)  $d=5.3 \mu\text{m}$ ; (d)  $d=2.0 \mu\text{m}$

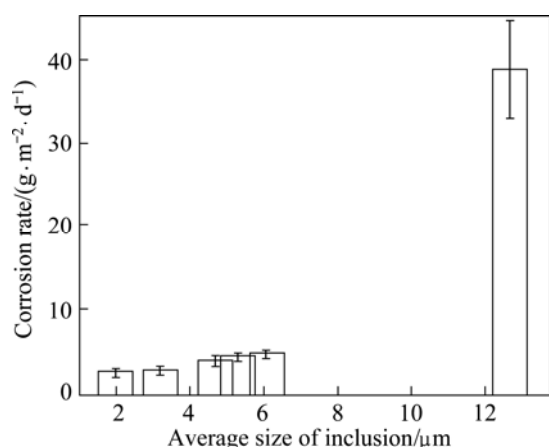


**Fig.5** Effect of average size of inclusions on corrosion rate of Mg-Gd-Y-Zr alloy

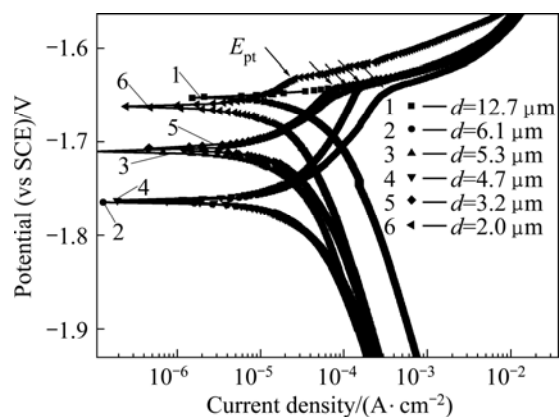


**Fig.6** Polarization curves of Mg-Gd-Y-Zr alloys with different average sizes of inclusions

average size of inclusions in the alloy while the corrosion rate decreases. From anodic side, the polarization curves of the alloys containing smaller inclusions exhibit a plateau. The plateau is limited by the breakdown potential ( $E_{\text{pt}}$ ), which corresponds to the crack of the protective film formed on the specimen. When the average size of inclusions in the alloys is smaller than  $12.7 \mu\text{m}$ , the breakdown potential is about  $-1.64 \text{ V}$ . However, the alloy with the average size of  $12.7 \mu\text{m}$  does not possess plateau, exhibiting poor corrosion behavior. For the alloys containing inclusions with average size smaller than  $12.7 \mu\text{m}$ , the current densities at the breakdown potential are listed in Table 1, and the results show that the anodic current densities increase with the increase of average size of inclusions. When the average size of inclusion reduces to  $2 \mu\text{m}$ , the current density decreases to the lowest value ( $20 \mu\text{A}/\text{cm}^2$ ). All the differences are caused by the different inclusion

**Table 1** Relationship between average size of inclusions and anodic current density

Average size of inclusion/ $\mu\text{m}$	Anodic current density/ $(\mu\text{A}\cdot\text{cm}^{-2})$
6.1	280
5.3	150
4.7	130
3.2	70
2.0	20

contents in the alloy by purification treatments. This modification in the polarization curve is well pronounced and reveals rather clearly the ability of purification treatment to impact electrochemical kinetics.

The relationship between polarization resistance and average size of inclusions in Mg-Gd-Y-Zr alloys is shown in Fig.7. The value of slope at corrosion potential represents the polarization resistance. Generally, the corrosion rate will decrease with increasing polarization resistance[18]. As shown in Fig.7, the polarization resistance of the alloys is enhanced as the average size of inclusions decreases. When the size of inclusions is less than 12.7  $\mu\text{m}$ , the polarization resistance will increase remarkably. However, when the size of inclusions is reduced to below 4.0  $\mu\text{m}$ , the polarization resistance tends to a constant value. The results indicate that there exists a critical average size of the inclusions to influence the polarization resistance, which is in accordance with the result of the salt spray test. Purification treatment can obtain apparent improvement in corrosion resistance.

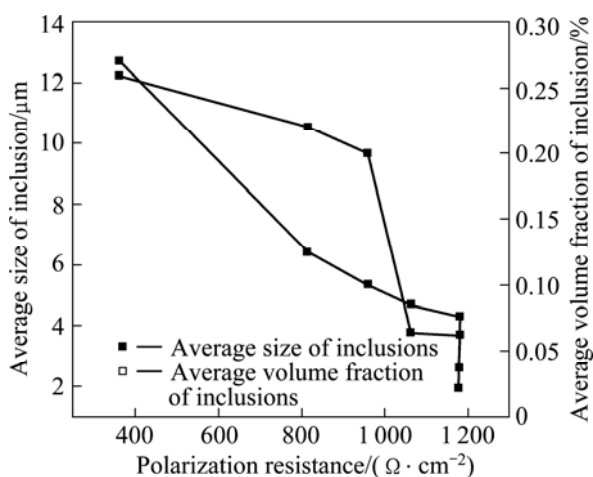


Fig.7 Effect of average size and volume fraction of inclusions on polarization resistance

## 4 Conclusions

1) Purification treatments can improve the purity of Mg-Gd-Y-Zr alloy. The method cannot only remove the large inclusions effectively but improve the distribution of the finer inclusions in the alloy. Under vacuum condition, the average size and volume fraction of the inclusions decrease to 2.0  $\mu\text{m}$  and 0.04%, respectively.

2) The corrosion rate of the alloy with purification treatment is decreased from 38.8  $\text{g}/(\text{m}^2 \cdot \text{d})$  to 2.4  $\text{g}/(\text{m}^2 \cdot \text{d})$  with the decrease of the average size of inclusions from 12.7  $\mu\text{m}$  to 2.0  $\mu\text{m}$ . The polarization resistance increases with decreasing the average size of inclusions in electrochemical tests, which indicates that anticorrosion ability is improved.

## References

- [1] HE S M, ZENG X Q, PENG L M, GAO X, NIE J F, DING Wen-jiang. Microstructure and strengthening mechanism of high strength Mg-10Gd-2Y-0.5Zr alloy [J]. Journal of Alloys and Compounds, 2007, 427(1-2): 316-323.
- [2] ANYANWU I A, KAMADO S, KOJIMA Y. Aging characteristics and high temperature tensile properties of Mg-Gd-Y-Zr alloys [J]. Materials Transaction, 2001, 42(7): 1206-1211.
- [3] WANG Bin, YANG Yuan-sheng, ZHOU Ji-xue, TONG Wen-hui. Effect of the pulsed magnetic field on the solidification and mechanical properties of Mg-Gd-Y-Zr alloy [J]. Rare Metal Material and Engineering, 2009, 38(3): 519-522.
- [4] STUMPHY B, MUDRYK Y, RUSSELL A, HERMAN D, GSCHNEIDNER K Jr. Oxidation resistance of B2 rare earth-magnesium intermetallic compounds [J]. Journal of Alloys and Compounds, 2008, 460(1-2): 363-367.
- [5] HU H, LUO A. Inclusions in molten magnesium and potential assessment techniques [J]. JOM, 1996, 48(10): 47-51.
- [6] JUNG H C, LEE Y C, SHIN K S. Fluxless recycling of die-cast AZ91 magnesium alloy scrap [J]. Materials Science Forum, 2005, 475-479: 541-544.
- [7] KITAHARA Y, SHIMAZAKI H, YABU T, NOGUCHI H, SAKAMOTO M, UENO H. Influence of inclusions on fatigue characteristics of non-combustible Mg alloy [J]. Materials Science Forum, 2005, 482: 359-362.
- [8] ZHANG L F, DUPONT T. State of the art in the refining and recycling of magnesium [J]. Materials Science Forum, 2007, 546-549: 25-36.
- [9] GAO Hong-tao, WU Guo-hua, DING Wen-jiang, ZHU Yan-ping. Purifying effect of new flux on magnesium alloy [J]. Trans Nonferrous Met Soc China, 2004, 14(3): 530-536.
- [10] BAKKE P, ENGH T A, BATHEN E, ØYMO D, NORDMARK A. Magnesium filtration with ceramic foam filters and subsequent quantitative microscopy of the filters [J]. Materials and Manufacturing Process, 1994, 9(1): 111-138.
- [11] HILLIS J E. Magnesium recycling: Flux versus flux-free processes principles, advantages and disadvantages [C]//Proceeding of the 64th Annual World Magnesium Conference. Vancouver, Canada, 2007: 55-66.
- [12] WU Guo-hua, SEUNG H K, BONG S Y, CHANG D Y. Effects of non-flux purification on the microstructure and mechanical properties of AZ31+xCa Mg alloy [J]. Materials Science Forum, 2007, 546-549: 217-220.
- [13] WANG Wei, HUANG Yu-guang, WU Guo-hua, WANG Qu-dong, SUN Ming, DING Wen-jiang. Influence of flux containing  $\text{YCl}_3$  additions on purifying effectiveness and properties of Mg-10Gd-3Y-0.5Zr alloy [J]. Journal of Alloys and Compounds, 2009, 480(2): 386-391.
- [14] WANG Wei, WU Guo-hua, WANG Qu-dong, HUANG Yu-guang, DING Wen-jiang. Gd contents, mechanical and corrosion properties of Mg-10Gd-3Y-0.5Zr alloy purified by fluxes containing  $\text{GdCl}_3$  additions [J]. Materials Science and Engineering A, 2009, 507(1-2): 207-214.
- [15] WANG Jie, ZHOU Ji-xue, TONG Wen-hui, YANG Yuan-sheng. Effect of purification treatment on properties of Mg-Gd-Y-Zr alloy [J]. Trans Nonferrous Met Soc China, 2010, 20(7): 1235-1239.
- [16] ASTM B117. Standard test method of salt spray testing [S]. 1990: 20-26.
- [17] GAO Hong-tao, WU Guo-hua, DING Wen-jiang, LIU Liu-fa, ZENG Xiao-qin, ZHU Yan-ping. Study on Fe reduction in AZ91 melt by  $\text{B}_2\text{O}_3$  [J]. Materials Science and Engineering A, 2004, 368(1-2): 311-317.
- [18] YE Xin-yu, CHEN Min-fang, YANG Meng, WEI Jun, LIU De-bao. In vitro corrosion resistance and cytocompatibility of nano-hydroxyapatite reinforced Mg-Zn-Zr composites [J]. J Mater Sci: Mater Med, 2010, 21: 1321-1328.

## 净化处理对 Mg-Gd-Y-Zr 镁合金耐蚀性的影响

王 杰, 杨院生, 童文辉

中国科学院 金属研究所, 沈阳 110016

**摘 要:** 在真空和非真空条件下对 Mg-Gd-Y-Zr 镁合金进行过滤净化处理。利用 OM 和 SEM 方法分析合金中夹杂物的种类、形貌、尺寸分布和体积分数; 利用盐雾实验和电化学测试研究 Mg-Gd-Y-Zr 镁合金中夹杂物对合金耐蚀性的影响。结果表明: 过滤净化处理可以有效地去除合金中的夹杂物; 通过净化处理, 合金中的夹杂物平均尺寸从 12.7  $\mu\text{m}$  减小到 2.0  $\mu\text{m}$ , 夹杂物的平均体积分数从 0.30% 降低到 0.04%; 随着合金中夹杂物尺寸的减小, 盐雾腐蚀实验中合金的腐蚀速率从 38.8  $\text{g}/(\text{m}^2\cdot\text{d})$  减少到 2.4  $\text{g}/(\text{m}^2\cdot\text{d})$ ; 在电化学实验中, 腐蚀电流密度减小, 极化电阻升高, Mg-Gd-Y-Zr 镁合金的耐蚀性得到了提高。

**关键词:** Mg-Gd-Y-Zr 镁合金; 过滤净化; 夹杂物; 腐蚀速率; 极化曲线; 极化电阻

(Edited by LI Xiang-qun)